Hindawi Publishing Corporation
International Journal of Photoenergy
Volume 2013, Article ID 289328, 7 pages
http://dx.doi.org/10.1155/2013/289328

Research Article

Mechanisms of Visible Light Photocatalysis in N-Doped Anatase TiO_2 with Oxygen Vacancies from GGA+U Calculations

Hsuan-Chung Wu,[1,2] Yu-Siang Lin,[1] and Syuan-Wei Lin[1]

[1] *Department of Materials Engineering, Ming Chi University of Technology, New Taipei 24301, Taiwan*
[2] *Center for Thin Film Technologies and Applications, Ming Chi University of Technology, New Taipei 24301, Taiwan*

Correspondence should be addressed to Hsuan-Chung Wu; hcwu@mail.mcut.edu.tw

Received 5 July 2012; Revised 15 January 2013; Accepted 16 January 2013

Academic Editor: Leonardo Palmisano

We have systematically studied the photocatalytic mechanisms of nitrogen doping in anatase TiO_2 using first-principles calculations based on density functional theory, employing Hubbard U (8.47 eV) on-site correction. The impurity formation energy, charge density, and electronic structure properties of TiO_2 supercells containing substitutional nitrogen, interstitial nitrogen, or oxygen vacancies were evaluated to clarify the mechanisms under visible light. According to the formation energy, a substitutional N atom is better formed than an interstitial N atom, and the formation of an oxygen vacancy in N-doped TiO_2 is easier than that in pure TiO_2. The calculated results have shown that a significant band gap narrowing may only occur in heavy nitrogen doping. With light nitrogen doping, the photocatalysis under visible light relies on N-isolated impurity states. Oxygen vacancies existence in N-doped TiO_2 can improve the photocatalysis in visible light because of a band gap narrowing and n-type donor states. These findings provide a reasonable explanation of the mechanisms of visible light photocatalysis in N-doped TiO_2.

1. Introduction

Photocatalytic mechanisms are created with an electron-hole pair by exciting an electron from the valence band to the conduction band through absorption of the electromagnetic radiation. Since the pioneering work of Fujishima and Honda in 1972 [1], titanium dioxide (TiO_2) has attracted attention as a photocatalytic material due to nontoxicity, low cost, and chemical stability. However, anatase TiO_2 has a wide band gap (3.2 eV) and only absorbs ultraviolet (UV) light at wavelengths shorter than 387 nm. UV light accounts for a small fraction (~5%) of solar energy impinging on the surface of the Earth; that is, solar energy utilization is low. Limitations due to the wide band gap make TiO_2 ineffective for many potential applications. Because visible light (400–700 nm) accounts for a large fraction (~45%), the modification of TiO_2 for extending optical absorption to the visible light region has become a thoroughly researched topic.

Since Asahi et al. [2] reported in 2001 that nitrogen doping enhances photocatalytic activity under visible light, TiO_2 has been doped with a variety of elements, such as N [3–10], C [11], B [12], P [13], Fe [14, 15], and La [16] to study photocatalytic activity under visible light with nitrogen doping proving effectiveness. Although the nitrogen doping is considered more effective and widely studied, the photocatalytic mechanisms under visible light are still debatable. Asahi et al. [2] indicated that the N 2p states hybridize with O 2p states that result in a narrowing of the band gap with the material becoming photoactive in the visible light region. However, other studies have supported the notion that N-doping does not cause a narrowing of the band gap of TiO_2 [3, 4]. For example, Irie et al. [4] considered that an isolated N 2p band above the valence band was responsible for the response to visible light. Oxygen vacancies induced by N-doping contributed to the absorption as well as photoactivity in the visible light region were also reported [17–19]. Valentin et al. [20] employed theoretical calculations to show that nitrogen doping led to a substantial reduction of energy costs to form oxygen vacancies in TiO_2. This suggested that nitrogen doping was likely to be accompanied by the formation of oxygen vacancies. Rumaiz et al. [21] indicated that the related defect level of oxygen vacancies was approximately 1 eV above

the valence band maximum (VBM) and explained the knee formation in the optical absorbance spectra of N-doped TiO_2. Lee et al. [22] suggested that the interstitial N-doping states with the oxygen deficiency were more effective for photocatalysis than the substitutional N-doping states with the oxygen deficiency. Zhao and Liu [23] have employed density functional theory (DFT) and adopted a $2 \times 1 \times 1$ supercell model to investigate the modification mechanism of N-doped anatase TiO_2. The calculated band gap of pure anatase TiO_2 was 2.68 eV, which was smaller than the experimental value of 3.2 eV, due to the limitation of DFT. The results have shown that except for oxygen deficient model, the band gaps of N-doped TiO_2, including substitutional and interstitial N-doping models, were narrowed between 0.03 and 0.23 eV. The fundamental absorption edges extended to the visible light region.

As mentioned above, the mechanisms of N-doping in TiO_2 under visible light region have three views: (1) band gap narrowing, (2) impurity energy levels, and (3) oxygen vacancies. Although theoretical calculations have been investigated for the mechanisms, most of them greatly underestimated the band gap of TiO_2 due to the adoption of conventional DFT method. In this paper, first-principles calculations employing the generalized gradient approximation (GGA) and Hubbard U approach are performed to investigate the formation energy, charge density, and electronic structure of N-doped anatase TiO_2 with oxygen vacancies systematically to comprehend the mechanisms of N-doped anatase TiO_2. The calculated results were analyzed and compared with the previous literature.

2. Calculation Models and Methods

A $2 \times 2 \times 1$ supercell of a pure anatase TiO_2 containing 16 Ti atoms and 32 O atoms was considered in this study as shown in Figure 1(a). To investigate the effect of the N-doping and oxygen vacancy in TiO_2 on the electronic structure, five defect types were modeled as shown in Figures 1(b)–1(f). The substitutional N-doping supercell (Figure 1(b)) was labeled N_s and constructed by substituting one oxygen atom with one nitrogen atom (2.1 at.%) and the interstitial N-doping supercell (Figure 1(c)) being labeled N_i, with one N atom was embedded into the interspace. In oxygen vacancy systems, one O atom was removed and were labeled O_v (Figure 1(d)), N_sO_v (Figure 1(e), with one O atom being substituted by N atom), and N_iO_v (Figure 1(f), with one N atom being embedded into the interspace).

First-principles calculations were performed using the CASTEP module [24] in Materials Studio 5.0 developed by Accelrys Software Inc. Electron-ion interactions were modeled using ultrasoft pseudopotentials in the Vanderbilt form [25]. The valence atomic configurations were $2s^22p^4$ for O, $2s^22p^3$ for N, and $3s^23p^63d^24s^2$ for Ti. The wave functions of the valence electrons were expanded through a plane wave basis set, and the cutoff energy was selected as 400 eV. The Monkhorst-Pack scheme [26] K-points grid sampling was set at $4 \times 4 \times 3$ (less than $0.04\ \text{Å}^{-1}$) in the supercells. The convergence threshold for self-consistent iterations was set at 5×10^{-6} eV. In the optimization process, the energy change, maximum force, maximum stress, and maximum displacement tolerances were set at 9×10^{-5} eV/atom, 0.09 eV/Å, 0.09 GPa, and 0.009 Å, respectively.

The spin-polarized GGA+U approach introduced an intra-atomic electron-electron interaction as an on-site correction to describe systems with localized d and f electrons capable of producing a more optimal band gap. Determination of an appropriate effective Hubbard U_{eff} parameter is necessary in GGA+U calculations to interpret the intra-atomic electron correlation correctly. As shown in Figure 2, for anatase TiO_2, the band gap widens when the effective Hubbard U_{eff} was increased. The band gap was effectively widened by increasing U_{eff} from 2 to 8 eV. Here, the effective on-site Coulomb interaction was $U_{\text{eff}} = 8.47$ eV for Ti 3d in the GGA+U approach and the calculated band gap of pure anatase is 3.21 eV, similar to the experimental value.

3. Results and Discussion

3.1. Formation Energy. To examine the relative stability of N-doped TiO_2 for various defective models, the defect formation energies (E_f) were calculated according to the following formula:

$$E_f = E_{\text{tot}}\,(\text{defect}) - E_{\text{tot}}\,(\text{pure}) - m\mu_{\text{N}} + n\mu_{\text{O}}. \quad (1)$$

E_{tot} (defect) and E_{tot} (pure) are the total energies of defective models and pure TiO_2; μ_{N} and μ_{O} represent the chemical potentials of the N and O atoms; m and n are the numbers of doped nitrogen and removed oxygen atoms; $m = 1$ and $n = 1$ for N_s model, and $m = 1$, $n = 0$ for N_i model, $m = 0$, $n = 1$ for O_v model, $m = 1$, $n = 2$ for N_sO_v model, $m = 1$, $n = 1$ for N_iO_v model. The formation energy depends on growth conditions and can be Ti-rich or O-rich. For TiO_2, μ_{Ti} and μ_{O} satisfy the relationship $\mu_{\text{Ti}} + 2\mu_{\text{O}} = \mu_{\text{TiO}_2}$. Under the O-rich growth condition, μ_{O} is determined by the total energy of an O_2 molecule ($\mu_{\text{O}} = \mu_{\text{O}_2}/2$) and μ_{Ti} is determined by the formula $\mu_{\text{Ti}} = \mu_{\text{TiO}_2} - 2\mu_{\text{O}}$. Under the Ti-rich growth condition, μ_{Ti} is the energy of one Ti atom in bulk Ti and μ_{O} is determined by $\mu_{\text{O}} = (\mu_{\text{TiO}_2} - \mu_{\text{Ti}})/2$.

It should be noted that the formation energy of a defective system depends on the selected U value. The U value of 8.47 eV was fixed to qualitatively examine the relative stability of N-doped TiO_2 for various defective models in this study. Table 1 summarizes the calculated formation energies for different defective models in TiO_2. The smaller E_f value represents that a defective system is more stable. The $E_f(N_s)$ (formation energy of N_s model) is smaller under the Ti-rich condition than that under O-rich condition, indicating that the incorporation of N into TiO_2 at the O site is thermodynamically favorable. At the Ti-rich condition, the $E_f(N_s)$ is smaller than $E_f(N_i)$, indicating that substitutional N atoms are more probable to be formed. This result is opposite with Zhao's calculated result (interstitial N atoms are favored) [23], but is consistent with Lee's calculated result [22]. It can be found that the formation energy of an oxygen vacancy from pure TiO_2 is 1.0 eV ($E_f(O_v) = 1.0$) and that from N_s-doped TiO_2 is 0.26 ($E_f(N_sO_v) - E_f(N_s)$). This represents that

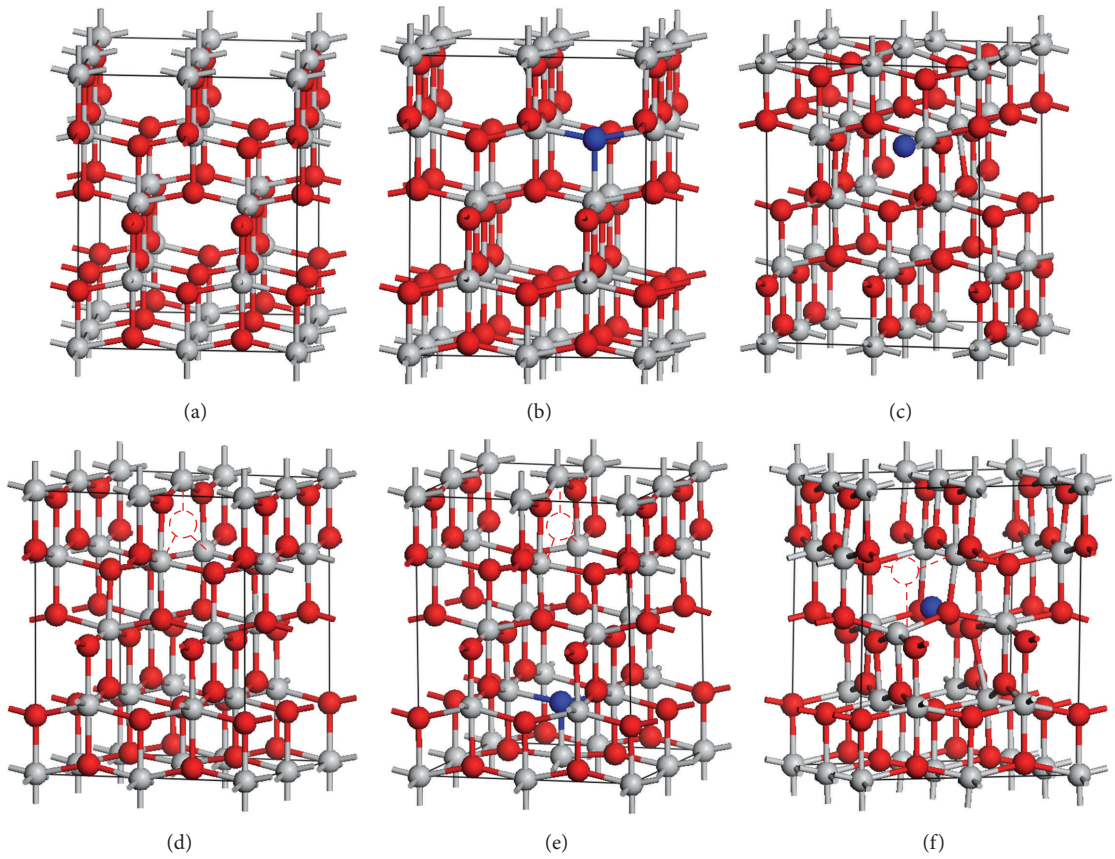

Figure 1: $2 \times 2 \times 1$ anatase TiO_2 supercell models: (a) pure TiO_2; (b) substitutional N-doping (N_s); (c) interstitial N-doping (N_i); (d) oxygen vacancy (O_v); (e) substitutional N-doping with oxygen vacancy (N_sO_v); and (f) interstitial N-doping with oxygen vacancy (N_iO_v). Gray, red, blue, and dotted line spheres represent Ti, O, and N atoms, and oxygen vacancy, respectively.

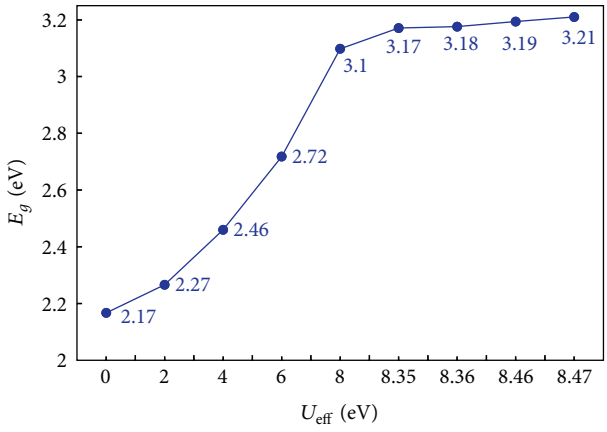

Figure 2: Relationship between the effective Hubbard parameter (U_{eff}) and the band gap (E_g) of anatase TiO_2.

the formation of oxygen vacancies with N existence in TiO_2 is easier than pure TiO_2 and is in agreement with the previous literature [21, 23].

3.2. Electronic Density. Table 1 summarizes Mulliken populations. Figure 3 indicates the charge distribution of each

Table 1: Formation energy and average Mulliken population of various defective models of N-doped TiO_2.

TiO_2	Formation energy		Mulliken population ($\|e\|$)		
Model	Ti-rich	O-rich	Ti	O	N
Pure			1.470	−0.730	
N_s	0.21	4.51	1.464	−0.737	−0.620
N_i	3.07	3.07	1.469	−0.728	−0.270
O_v	1.00	5.30	1.435	−0.744	
N_sO_v	0.47	9.07	1.435	−0.741	−0.750
N_iO_v	4.18	8.48	1.419	−0.726	−0.180

defective model of N-doped TiO_2. For pure TiO_2, the average population values of Ti and O atoms are 1.47 and −0.73. The Ti atom has a much higher population value which indicates that a large oxidation occurred. For N_s model, Table 1 shows that the Mulliken population of N_s (−0.62) is larger than that of O (−0.737) and leads to an unfilled 2p orbital in the N atom because the electronegativity of N is lower than that of O as shown in Figure 3(a). For N_i model, the Mulliken population of N_i is −0.27, indicating that the N_i atom obtains fewer electrons from Ti atoms. Figure 3(b) shows that the charge is shared between the N_i atom and its neighbor O

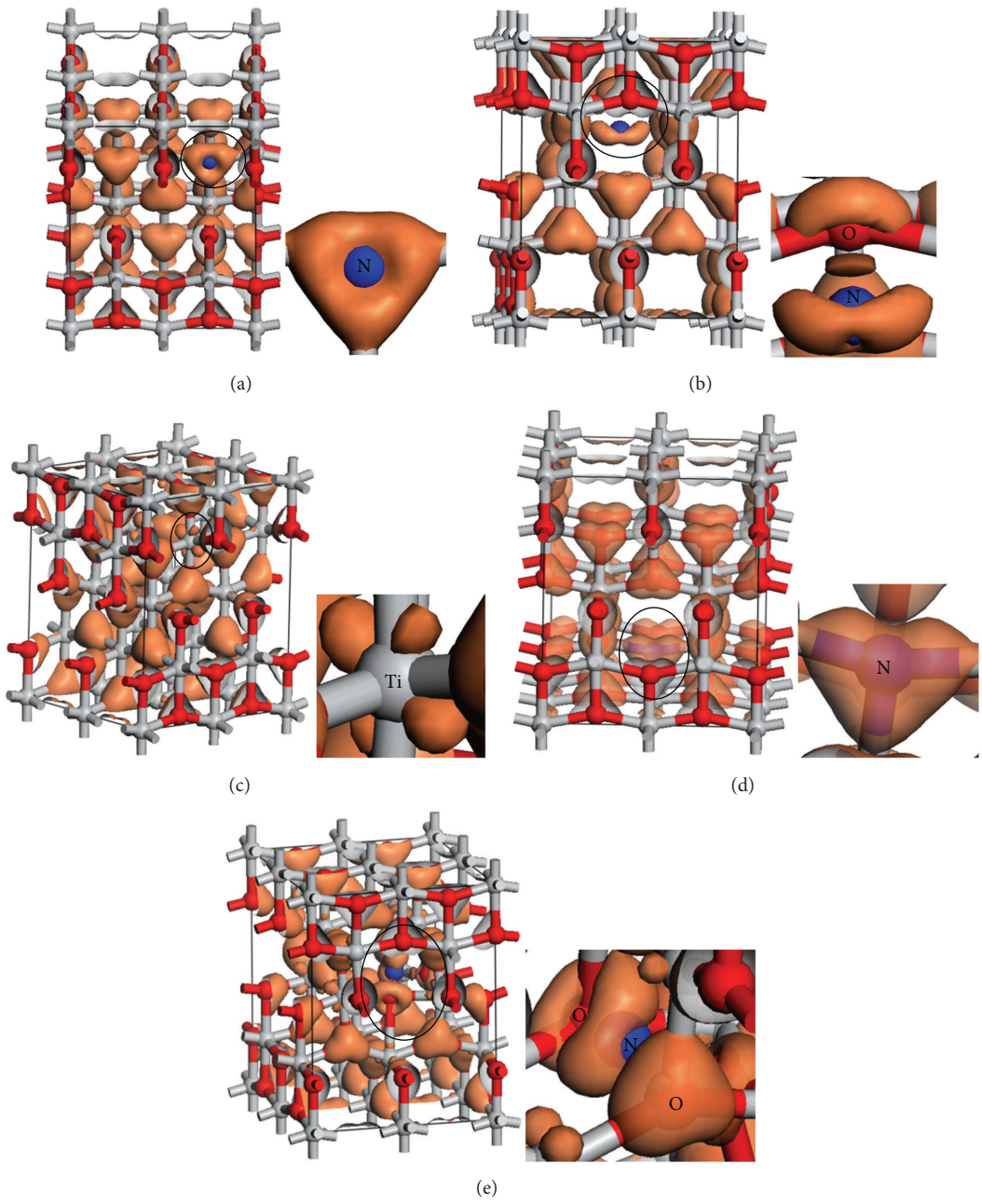

Figure 3: Charge distribution of various defective models in N-doped TiO_2: (a) N_s, (b) N_i, (c) O_v, (d) N_sO_v, and (e) N_iO_v.

atom and the similar results were reported by Rumaiz et al. [21]. For O_v model, as caused by two extra electrons after removing an oxygen atom, the Mulliken populations of Ti and O (1.435 and −0.744) are both smaller than in the pure model and lead to more electrons in Ti and O atoms. Figure 3(c) shows that the electrons are remained in a Ti atom near the oxygen vacancy. Comparing the N_s with N_sO_v models, the Mulliken population of N atom decreases from −0.62 to −0.75, indicating that there are more electrons that transfer from oxygen vacancy to the N atom, and the N 2p orbital is filled as shown in Figure 3(d). For N_iO_v model, the electron clouds are shared between N_i and the adjacent O atoms. They increase the population values in N_i and O atoms.

3.3. Electronic Structure. Figure 4 indicates the total density of states (TDOS), and the projected density of states (PDOS) of various defective models was calculated to investigate the electronic properties of N-doped anatase TiO_2. Other related values that were calculated include the band gap (E_g), the width of the valence band (W_{VB}), and the maximum absorption wavelength ($\lambda_{max} = 1240/E_g$) that Table 2 summarizes. The band gap (E_g) of pure anatase TiO_2 is 3.21 eV as shown in Figure 4(a) and is consistent with the experimental value of

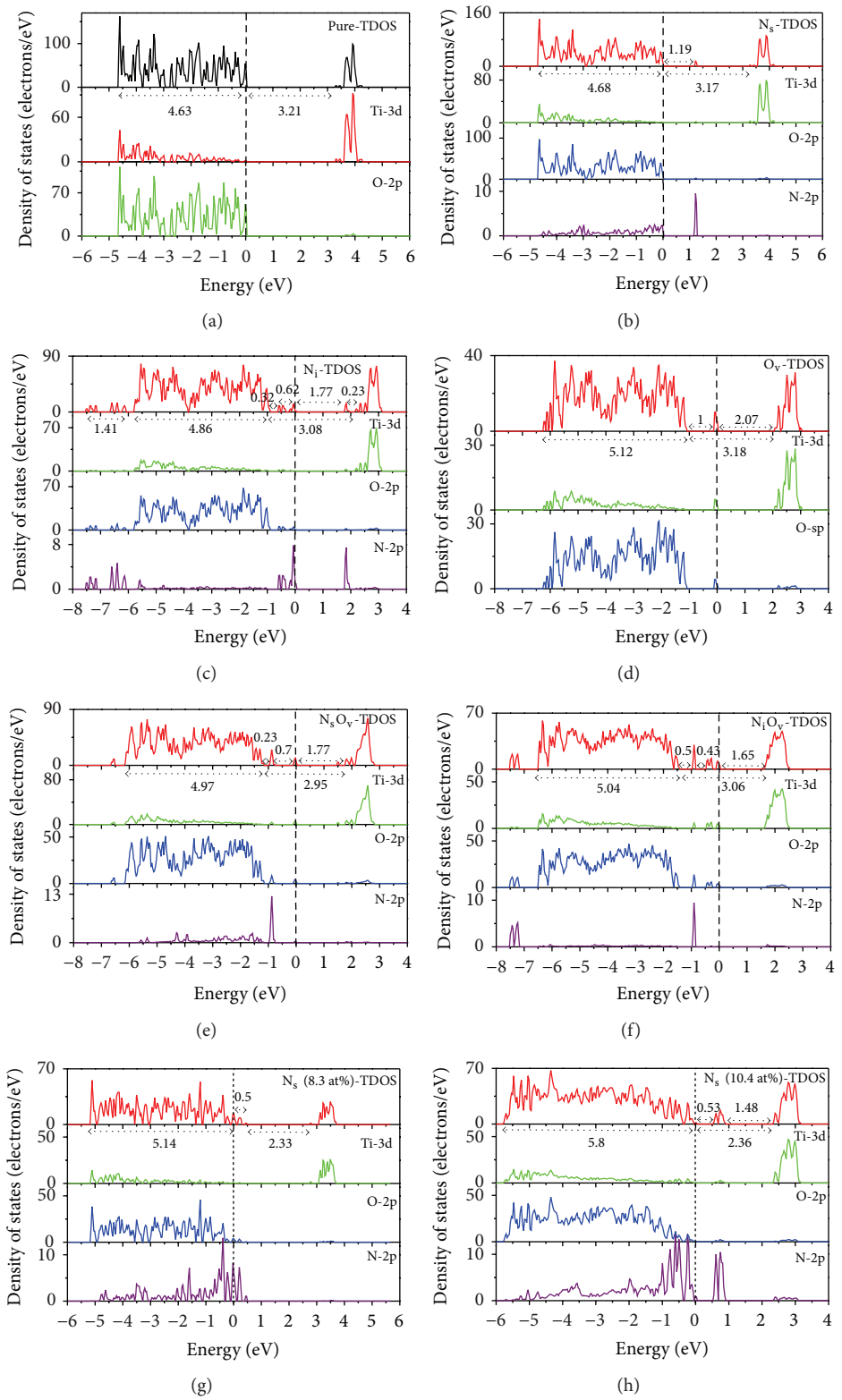

FIGURE 4: DOS of various defective models of N-doped TiO_2: (a) pure TiO_2, (b) N_s (2.1 at.%), (c) N_i, (d) O_v, (e) N_sO_v, (f) N_iO_v, (g) N_s (8.3 at.%), and (h) N_s (10.4 at.%).

Table 2: Band gap, maximum absorption, wavelength, and width of valence band for various defective models of N-doped TiO_2.

Model	E_g (eV)	λ_{max} (nm)	W_{VB} (eV)
Pure	3.21	386	4.63
N_s (2.1 at.%)	3.17	391	4.68
N_i	3.08	402	4.86
O_v	3.18	390	5.12
N_sO_v	2.95	420	4.97
N_iO_v	3.06	405	5.04
N_s (8.3 at.%)	2.33	532	5.14
N_s (10.4 at.%)	2.36	525	5.80

3.2 eV. The valence band of TiO_2 has a large bandwidth (W_{VB}) of approximately 4.63 eV, showing a strong delocalization among the O 2p electrons. For N_s model from Figure 4(b), the E_g gap is 3.17 eV and the W_{VB} is 4.68 eV, implying that E_g and W_{VB} are not changed obviously compared with the pure TiO_2. It is demonstrated from Figure 4(b) that one isolated N 2p state is localized above the top of the VB of the host TiO_2 and is consistent with the calculations of Long [27]. The electron in the VB is excited to localized impurity states in the band gap and subsequently to the CB through absorption of visible light. For N_i model from Figure 4(c), the E_g is narrowed to 3.08 eV and the W_{VB} is broadened to 4.86 eV. It was observed that the N 2p states primarily contributed to three energy ranges: −7.5 to −6.1, −0.6 to 0, and 1.8 to 2 eV. For O_v model from Figure 4(d), the E_g (3.18 eV) is not changed obviously and the W_{VB} is broadened to 5.12 eV. The two extra electrons resulted from removing an oxygen atom lead to an occupied state near Fermi energy level and are localized at 1.0 eV above the top of VB and consistent with the experimental results [21]. Comparing with the N_s and N_i models, both band gaps of the N_sO_v and N_iO_v (2.95 and 3.06 eV) became smaller and extended optical absorption into the visible region (420 and 405 nm). Figures 4(e)-4(f) show that the W_{VB} became broader. Therefore, the existence of oxygen vacancies in N-doped anatase TiO_2 improves the photocatalysis under visible light. Our previous work regarding DOS for heavy nitrogen doping in the N-doped anatase TiO_2 are shown in Figures 4(g)-4(h) [8]. It can be observed that a significant narrowing of the band gap of N-doped TiO_2 occurs only for heavy nitrogen doping (≥8.3 at.%) and is in agreement with Ashai calculated results [2]. As a result, the electron transition energy from the valence band to the conduction band decreased by approximately 0.88 eV because of the heavy nitrogen doping and, thus, may induce a red shift (extending to 532 nm) at the edge of the optical absorption range. Both the narrowing of the band gap and the increased mobility of photo-generated carriers in heavy nitrogen doping concentrations improve the photocatalytic activity under visible light, as illustrated in recent experimental results [6, 7].

4. Conclusions

Using the GGA+U method, this study calculated impurity formation energy, charge density, and electronic properties of an N-doped anatase TiO_2 with oxygen vacancies system to investigate the photocatalytic mechanisms of N-doped TiO_2 under visible light. An effective Hubbard U of 8.47 eV was adopted to determine the experimental band gap correctly. The formation energy calculated results have shown that the substitutional N atom was easier to be formed than the interstitial one and the formation of oxygen vacancies under nitrogen existence in TiO_2 was easier to be formed than pure TiO_2. The calculated results have shown that the mechanisms of photocatalytic activity under visible light are concluded as the following: (1) the significant band gap narrowing may occur in heavy nitrogen doping; (2) with light nitrogen doping, the mechanism is the result of N-isolated impurity states; and (3) oxygen vacancies existence in N-doped TiO_2 improves the photocatalysis in visible light because of a band gap narrowing and n-type donor states.

Acknowledgments

This work was supported by the National Science Council in Taiwan (NSC 101-2221-E-131-022), for which the authors are grateful. The authors also acknowledge the National Center for High-Performance Computing for computer time and the use of its facilities.

References

[1] A. Fujishima and K. Honda, "Electrochemical photolysis of water at a semiconductor electrode," *Nature*, vol. 238, no. 5358, pp. 37–38, 1972.

[2] R. Asahi, T. Morikawa, T. Ohwaki, K. Aoki, and Y. Taga, "Visible-light photocatalysis in nitrogen-doped titanium oxides," *Science*, vol. 293, no. 5528, pp. 269–271, 2001.

[3] Y. Nakano, T. Morikawa, T. Ohwaki, and Y. Taga, "Deep-level optical spectroscopy investigation of N-doped TiO_2 films," *Applied Physics Letters*, vol. 86, no. 13, Article ID 132104, 3 pages, 2005.

[4] H. Irie, Y. Watanabe, and K. Hashimoto, "Nitrogen-concentration dependence on photocatalytic activity of $TiO_{2-x}N_x$ powders," *Journal of Physical Chemistry B*, vol. 107, no. 23, pp. 5483–5486, 2003.

[5] B. Liu, L. Wen, and X. Zhao, "The structure and photocatalytic studies of N-doped TiO_2 films prepared by radio frequency reactive magnetron sputtering," *Solar Energy Materials and Solar Cells*, vol. 92, no. 1, pp. 1–10, 2008.

[6] P. G. Wu, C. H. Ma, and J. K. Shang, "Effects of nitrogen doping on optical properties of TiO_2 thin films," *Applied Physics A*, vol. 81, no. 7, pp. 1411–1417, 2005.

[7] X. Jiang, Y. Wang, and C. Pan, "High concentration substitutional N-doped TiO_2 film: preparation, characterization and photocatalytic property," *Journal of the American Ceramic Society*, vol. 94, no. 11, pp. 4078–4083, 2011.

[8] H. C. Wu, S. W. Lin, and J. S. Wu, "Effects of nitrogen concentration on N-doped anatase TiO_2: density functional theory and Hubbard U analysis," *Journal of Alloys and Compounds*, vol. 522, pp. 46–50, 2012.

[9] G. Shang, H. Fu, S. Yang, and T. Xu, "Mechanistic study of visible-light-induced photodegradation of 4-chlorophenol by $TiO_{2-X}N_X$ with low nitrogen concentration," *International Journal of Photoenergy*, vol. 2012, Article ID 759306, 9 pages, 2012.

[10] J. Qian, G. Cui, M. Jing, Y. Wang, M. Zhang, and J. Yang, "Hydrothermal synthesis of nitrogen-doped titanium dioxide and evaluation of its visible light photocatalytic activity," *International Journal of Photoenergy*, vol. 2012, Article ID 198497, 6 pages, 2012.

[11] H. Yang and C. Pan, "Synthesis of carbon-modified TiO_2 nanotube arrays for enhancing the photocatalytic activity under the visible light," *Journal of Alloys and Compounds*, vol. 501, no. 1, pp. L8–L11, 2010.

[12] J. Zheng, Z. Liu, X. Liu, X. Yan, D. Li, and W. Chu, "Facile hydrothermal synthesis and characteristics of B-doped TiO_2 hybrid hollow microspheres with higher photo-catalytic activity," *Journal of Alloys and Compounds*, vol. 509, no. 9, pp. 3771–3776, 2011.

[13] Y. Lv, L. Yu, H. Huang, H. Liu, and Y. Feng, "Preparation, characterization of P-doped TiO_2 nanoparticles and their excellent photocatalystic properties under the solar light irradiation," *Journal of Alloys and Compounds*, vol. 488, no. 1, pp. 314–319, 2009.

[14] L. Wen, B. Liu, X. Zhao, K. Nakata, T. Murakami, and A. Fujishima, "Synthesis, characterization, and photocatalysis of Fe-doped TiO_2: a combined experimental and theoretical study," *International Journal of Photoenergy*, vol. 2012, Article ID 368750, 10 pages, 2012.

[15] M. C. Wang, H. J. Lin, C. H. Wang, and H. C. Wu, "Effects of annealing temperature on the photocatalytic activity of N-doped TiO_2 thin films," *Ceramics International*, vol. 38, no. 1, pp. 195–200, 2012.

[16] W. Chen, P. Yuan, S. Zhang, Q. Sun, E. Liang, and Y. Jia, "Electronic properties of anataseTiO_2 doped by lanthanides: A DFT + U study," *Physica B*, vol. 407, no. 6, pp. 1038–1043, 2012.

[17] Z. Lin, A. Orlov, R. M. Lambert, and M. C. Payne, "New insights into the origin of visible light photocatalytic activity of nitrogen-doped and oxygen-deficient anatase TiO_2," *Journal of Physical Chemistry B*, vol. 109, no. 44, pp. 20948–20952, 2005.

[18] M. Batzill, E. H. Morales, and U. Diebold, "Influence of nitrogen doping on the defect formation and surface properties of TiO_2 rutile and anatase," *Physical Review Letters*, vol. 96, no. 2, 4 pages, 2006.

[19] V. N. Kuznetsov and N. Serpone, "On the origin of the spectral bands in the visible absorption spectra of visible-light-active TiO_2 specimens analysis and assignments," *Journal of Physical Chemistry C*, vol. 113, no. 34, pp. 15110–15123, 2009.

[20] C. Di Valentin, G. Pacchioni, A. Selloni, S. Livraghi, and E. Giamello, "Characterization of paramagnetic species in N-doped TiO_2 powders by EPR spectroscopy and DFT calculations," *Journal of Physical Chemistry B*, vol. 109, no. 23, pp. 11414–11419, 2005.

[21] A. K. Rumaiz, J. C. Woicik, E. Cockayne, H. Y. Lin, G. H. Jaffari, and S. I. Shah, "Oxygen vacancies in N doped anatase TiO_2: experiment and first-principles calculations," *Applied Physics Letters*, vol. 95, no. 26, Article ID 262111, 3 pages, 2009.

[22] S. H. Lee, E. Yamasue, H. Okumura, and K. N. Ishihara, "Effect of oxygen and nitrogen concentration of nitrogen doped TiO_x film as photocatalyst prepared by reactive sputtering," *Applied Catalysis A*, vol. 371, no. 1-2, pp. 179–190, 2009.

[23] Z. Zhao and Q. Liu, "Mechanism of higher photocatalytic activity of anatase TiO_2 doped with nitrogen under visible-light irradiation from density functional theory calculation," *Journal of Physics D*, vol. 41, no. 2, Article ID 025105, 10 pages, 2008.

[24] M. D. Segall, P. J. D. Lindan, M. J. Probert et al., "First-principles simulation: ideas, illustrations and the CASTEP code," *Journal of Physics Condensed Matter*, vol. 14, no. 11, pp. 2717–2744, 2002.

[25] D. Vanderbilt, "Soft self-consistent pseudopotentials in a generalized eigenvalue formalism," *Physical Review B*, vol. 41, no. 11, pp. 7892–7895, 1990.

[26] H. J. Monkhorst and J. D. Pack, "Special points for Brillonin-zone integrations," *Physical Review B*, vol. 13, no. 12, pp. 5188–5192, 1976.

[27] R. Long and N. J. English, "First-principles calculation of synergistic (N, P)-codoping effects on the visible-light photocatalytic activity of anatase TiO_2," *Journal of Physical Chemistry C*, vol. 114, no. 27, pp. 11984–11990, 2010.